POLITECNICO DI TORINO
Repository ISTITUZIONALE

T-stress effects on crack deflection: Straight vs. curved crack advance

Original
T-stress effects on crack deflection: Straight vs. curved crack advance / Sapora, ALBERTO GIUSEPPE; Cornetti, Pietro; Manti, V.. - In: EUROPEAN JOURNAL OF MECHANICS. A, SOLIDS. - ISSN 0997-7538. - 60:(2016), pp. 52-57. [10.1016/j.euromechsol.2016.06.002]

Availability:
This version is available at: 11583/2652869 since: 2020-04-26T11:31:53Z

Publisher:
Elsevier Ltd

Published
DOI:10.1016/j.euromechsol.2016.06.002

Terms of use:

This article is made available under terms and conditions as specified in the corresponding bibliographic description in the repository

Publisher copyright
Elsevier postprint/Author's Accepted Manuscript

© 2016. This manuscript version is made available under the CC-BY-NC-ND 4.0 license http://creativecommons.org/licenses/by-nc-nd/4.0/.The final authenticated version is available online at: http://dx.doi.org/10.1016/j.euromechsol.2016.06.002

(Article begins on next page)

12 October 2024

T-stress effects on crack deflection: straight vs. curved crack advance

A. Sapora , P. Cornetti , V. Mantič

Department of Structural, Geotechnical and Building Engineering, Politecnico di Torino, Corso Duca degli Abruzzi 24, 10129, Torino, Italy

Group of Elasticity and Strength of Materials, School of Engineering, Universidad de Sevilla, Camino de los Descubrimientos s/n, 41092, Sevilla, Spain

Abstract

T-stress effects on crack deflection in notched brittle materials are investigated by means of an average stress approach. It is shown that the crack advance always reveals to be straight if the T contribution is negligible. On the contrary, if T is different from zero, the trajectory tends to curve: the higher is $|T|$, the larger is the curvature parameter, its value being either positive or negative depending on the sign of T. Analogies and differences with respect to straight crack propagation are quantified in terms of the fracture loci and of the critical kinking angle. The investigation on the stability of crack deflection under mode I loading conditions concludes the paper, together with a discussion on experimental observations.

Keywords: average circumferential stress, T-stress, curved crack advance, mode I stability

Email address: alberto.sapora@polito.it, pietro.cornetti@polito.it, mantic@us.es (A. Sapora , P. Cornetti , V. Mantič)

1. Introduction

The classical stress intensity factors (SIFs) govern the singular stress field in the neighborhood of the notch root, whereas higher order terms in William's asymptotic expansion affect the stress solution only at a certain distance from the crack tip. The first non-singular term is known as T-stress, which represents the constant term parallel to the crack plane. Indeed, its effects on crack deflection in homogenous brittle materials have been widely investigated since the beginning of sixties. Several different models were proposed by imposing either a strain statement, a stress threshold, an energy condition, or by coupling both a stress requirement and the energy balance (Erdogan and Sih, 1963; Cotterell, 1972; Williams and Ewing, 1972; Finnie and Saith, 1973; Carpinteri et al., 1979; He et al., 1991; Becker et al., 2001; Smith et al., 2001, 2006; Leguillon and Murer, 2008; Cornetti et al., 2014; Gupta et al., 2015; Sapora and Mantič, 2016). From the above studies, it emerges clearly that T-stress affects both the apparent fracture toughness and the critical kinking angle. Furthermore, T-influence reveals to be more significant for prevailing mode II conditions and as less brittle materials are considered. A special mention deserve geometries where the SIFs are both null, e.g. large plane slabs under remote uniaxial traction with a central through thickness crack collinear to the force direction (Williams and Ewing, 1972; Carpinteri et al., 1979), where T governs the whole stress solution.

As concerns the case of pure mode I cracks under biaxial loading, Cotterell and Rice (1980) proposed in their pioneering work, by a first-order perturbation scheme of complex potentials, that for $T < 0$ the crack path is always stable, whereas for $T > 0$ the propagation reveals to be unstable. Indeed, similar results had been obtained even before by Banichuk (1970); Goldstein and Salganik

(1970) through an analogous procedure. The dependence of the crack path stability only upon the sign of T-stress was object of a heated scientific discussion, rising from experimental tests showing the presence of a positive threshold $T_{th} > 0$ above which instability occurs (Sumi et al., 1985; Selvarathinam and Goree, 1998; Chao et al., 2001). The problem was investigated by several studies: the point stress method was firstly exploited to evaluate T_{th} by Smith et al. (2001). On the basis of the studies presented in Broberg (1999), Melin (2002) pointed out that a critical role of the sign of the T-stress applies only to the situation of a single crack growing in a large plate and cannot be transferred to other situations directly. Leguillon and Murer (2008) evaluated T_{th} on the basis of the coupled criterion by Leguillon (2002). Focusing the attention on the T-stress variation after a small extension of the main crack (Li and Xu, 2007), Li et al. (2010) assumed that for positive T the crack firstly propagates in a stable manner until a critical crack growth distance, and then unstable propagation occurs. The estimate of T_{th} according to Finite Fracture Mechanics (FFM, Cornetti et al. (2014); Sapora and Mantič (2016)) differs somewhat from that by Leguillon and Murer (2008), although the two approaches provide a similar qualitative behavior. The strain energy density criterion predicts a value of T_{th} dependent also on the material Poisson's ratio (Ayatollahi et al., 2016). Finally, the role of T-stress on crack path is still object of investigation in the framework of dynamic propagation and of thermally driven fracture processes in quenched glass plates, although it seems unable to predict stability (Jayadevan et al., 2001; Yang and Ravi-Chandar, 2001).

Most of the approaches cited above refer to kinked or slightly curved cracks, which however were treated as perturbed straight cracks. Nevertheless, the presence of the curvature of the fracture plane was often detected experimentally,

even under mode I loading conditions(Radon et al., 1977; Ayatollahi et al., 2016): Radon et al. (1977) observed that ignoring the crack curvature for kinking angles up to 30° introduces errors of about 7% on the related failure load. The deviation increases up to 20% for angles close to 50°. Among the few (at least theoretical) attempts that were made to take the curvature into account, let us mention that by Karihaloo et al. (1981), who extended the first order perturbation scheme mentioned above to the second order perturbation approach, coming yet to the same conclusions by Cotterell and Rice (1980) on crack growth stability, and the subsequent works by Kariahaloo (1982); Sumi et al. (1985); Amestoy and Leblond (1992); Broberg (1999); Salvadori (2008).

In the present paper, all these concepts will be revisited through the average stress criterion proposed by Seweryn (1998). The approach lies in the framework of the Theory of Critical Distances (Taylor, 2007), stating that failure takes place when a mechanical quantity (in this case the average circumferential stress) at a finite distance from the crack tip reaches a critical value. The finite distance (also known as crack extension or crack advance) results to be a material function, depending on the tensile strength σ_u and the fracture toughness K_{Ic}. For the sake of simplicity, the crack advance will be assumed of type $y_1 \sim x_1^{3/2}$, (x_1, y_1) being the frame of reference obtained by rotating the cartesian system (x, y) by an angle γ (Fig. 1). The above function represents a simplified form of the one considered by Amestoy and Leblond (1992) (see also (Kariahaloo, 1982; Sumi et al., 1985)), where it was stated that this shape must be necessarily assumed if the extensions are to be obtainable by crack propagation and not by arbitrary machining of the body. Before proceeding, it is important to underline that the present analysis will focus on the first crack advance stemming from the notch tip and it will not

describe the complete crack path.

2. Average stress criterion

According to the average stress criterion, failure takes place when the average circumferential stress $\sigma_{\theta\theta}$ over a segment of length Δ equals the tensile strength σ_u. Differently from FFM (Carpinteri et al., 2011), where the crack advance depends also on the geometrical features thus resulting to be a structural parameter, here Δ depends merely on the material properties and it can be expressed as:

$$\Delta = \frac{2}{\pi}\left(\frac{K_{Ic}}{\sigma_u}\right)^2 = \frac{2}{\pi} l_{ch}, \tag{1}$$

l_{ch} being the well-known Irwin's length. The value of Δ expressed by Eq.(1) is not arbitrary, but it must be necessarily assumed in order to provide the Linear Elastic Fracture Mechanics (or Griffith) relationship $K_I = K_{Ic}$ for a mode I specimen containing a sufficiently large crack. On the other hand, when comparing theoretical predictions with experimental results, the value of σ_u (and thus of Δ) is often fitted for some materials, such as polymers and metals. As a matter of fact, the experimental estimation on σ_u when testing plain specimens is strongly affected by the presence of micro-cracks/defects, and by crazing or plasticity phenomena (see, for instance, Taylor (2007)).

Although the stress criterion dates back to Neuber (1958) and Novozhilov (1969), it was formalized to V-notched elements under mode I loading conditions by Seweryn (1994), who later extended the approach to take T-stress effects and mixed-mode loading conditions into account (Seweryn, 1998; Seweryn and Lukaszewicz, 2002). Afterwards, several researchers applied this criterion over a wide range of geometries and materials (Taylor et al., 2004; Priel et al., 2007;

Ayatollahi and Torabi, 2010; Carpinteri et al., 2012; Sapora et al., 2013, 2014; Ayatollahi et al., 2015).

Let us recall the expression for the circumferential stress field in polar coordinates:

$$\sigma_{\theta\theta}(r,\theta) = \frac{K_I}{\sqrt{2\pi r}} f^I_{\theta\theta}(\theta) + \frac{K_{II}}{\sqrt{2\pi r}} f^{II}_{\theta\theta}(\theta) + T\sin^2\theta, \tag{2}$$

where K_I and K_{II} are the SIFs related to the parent (or mother) crack, $f^I_{\theta\theta}$ and $f^{II}_{\theta\theta}$ are the corresponding angular functions

$$f^I_{\theta\theta}(\theta) = \cos^3(\theta/2) \qquad f^{II}_{\theta\theta}(\theta) = -3\sin(\theta/2)\cos^2(\theta/2), \tag{3}$$

whereas the last term represents the T-stress contribution.

It is important also to remind that the relationships linking the cartesian frame of reference (x,y) to the polar frame of reference (r,θ) can be expressed as

$$\begin{cases} \theta = & \arctan\left(\frac{y}{x}\right) \\ r = & \sqrt{x^2+y^2} \end{cases} \tag{4}$$

.

The rotated frame of reference (x_1,y_1) is related to the cartesian frame of reference (x,y) by means of

$$\begin{cases} x = & x_1\cos(\gamma) - y_1\sin(\gamma) \\ y = & x_1\sin(\gamma) + y_1\cos(\gamma) \end{cases} \tag{5}$$

2.1. Straight crack propagation

Let us firstly assume that the kinked crack propagates (at least at the first step) straightly. By referring to Fig. 1 and imposing $a = 0$, the following conditions are

satisfied: $\theta \equiv \gamma$, $r \equiv x_1$, $y_1 = 0$. The average stress criterion can be expressed as:

$$\frac{1}{\Delta}\int_0^{\Delta} \sigma_{\theta\theta}(r,\theta)\mathrm{d}r = \sigma_u \tag{6}$$

Substituting Eqs. (1) and (2) into (6) and supposing that failure takes place when K_I reaches its critical value K_{If} , yields:

$$\frac{K_{If}}{K_{Ic}} = \frac{1}{f^I_{\theta\theta} + f^{II}_{\theta\theta}\tan\psi + \tau\sin^2\theta\sqrt{1+\tan^2\psi}}, \tag{7}$$

where the mode mixity ψ is defined as $\tan\psi = K_{II}/K_I$ and τ represents the dimensionless T-stress $\tau = T\sqrt{l_{ch}}/\sqrt{K_I^2 + K_{II}^2}$ (also known as biaxiality ratio, (Leevers and Radon, 1982; Smith et al., 2001)). Once the loading conditions and the structural properties (i.e., the geometry and the material) are given, the θ-value which maximizes the denominator at the right-hand side of Eq. (7) represents the critical kinking angle θ_c. The corresponding value provides the critical mode I SIF K_{If}. Results are presented in Figs. 2 and 3 as concerns the critical kinking angle and the fracture loci, respectively. As it is expected, negative T-values decrease the circumferential stress $\sigma_{\theta\theta}$: both the failure load and the negative kinking angle increase. An opposite trend is recovered for positive T-stresses. Observe that for sufficiently high $T > 0$, the crack ceases to propagate collinearly under mode I loading conditions ($\psi = 0°$) and the corresponding critical mode I SIF deviates from the fracture toughness K_{Ic}. This point will be discussed in details in Section 3.

Similar curves to those depicted in Fig. 2 and 3 were obtained by implementing different fracture criteria, from the point stress model (Smith et al., 2001), which in this case provides identical predictions to those by the present average approach, to FFM (Cornetti et al., 2014), where a different definition of τ was

adopted.

2.2. Curved crack propagation

Let us now suppose that fracture propagates (at least at the first step) by a curved crack advance described by the function $y_1 = ax_1^{\frac{3}{2}}$ (Fig. 1), a being a curvature parameter. The crack path can be described in parametric form as $\Gamma(t) = (t, at^{\frac{3}{2}})$, and the average stress criterion (6) can be recast as:

$$\frac{1}{\Delta}\int_{\Gamma}\sigma_{\theta\theta}ds = \frac{1}{\Delta}\int_0^{t_1}\sigma_{\theta\theta}(r(t),\theta(t))\sqrt{1+\frac{9}{4}a^2t}dt = \sigma_u \tag{8}$$

with

$$t_1 = \frac{4}{9a^2}\left[\left(\frac{27}{8}a^2\Delta+1\right)^{\frac{2}{3}}-1\right] \tag{9}$$

Upon substitution of Eqs. (4) and (5) into the stress field (2), and of the corresponding expression into Eq. (8) it is possible to get a solution for the problem under investigation. The procedure consists in looking for the couple of critical parameters (a_c, γ_c) which minimizes the fracture load (i.e., K_{If}). Equation (8) together with (9) were solved numerically and results were then interpolated by means of spline functions.

From Fig.3 it can be seen that if T is different from zero, the curved crack always corresponds to a lower failure load with respect to the straight case. The difference is more appreciable for higher $|\tau|$. As concerns the curvature parameter a, it is a monotonic function in $|\tau|$ and the dimensionless curves in Fig.4 show that: i) for negative T-stress, a is always positive. As a function of ψ, it increases from zero to a maximum (represented by circles in Fig.4), and then it decreases smoothly; ii) a is always negative for positive T-values. It attains a minimum in the neighborhood of mode I ($\psi \leq 10°$) and then it increases monotonically. As

mode II loading conditions are approached ($\psi \to 90°$), the difference between τ-curves decreases. Thus, positive T-stresses influence more the curvature under prevailing mode I conditions ($0° \leq \psi \leq 45°$), whereas it can be generally said that negative T affect more the curvature under prevailing mode II loading conditions ($45° \leq \psi \leq 90°$).

Finally, the critical kinking angle for various ψ and τ is represented in Fig. 5. The difference observed for both positive and negative T-values is not so significant when compared to the null T-stress. Indeed, the following explanation can be provided: the angle is governed by the parent mode mixity, as the T stress is negligible in comparison with singular stresses of the parent crack. On the other hand, as commented above, the kink curvature is strongly controlled by T stress which has influence on the kink-part more distant from the parent crack tip. Note also that the crack advance tends to curve (but not to kink, $\gamma_c = 0°$) for sufficiently high τ even under mode I loading conditions ($\psi = 0°$).

In Table 1 the dimensionless d/l_{ch} distance between the end points of the crack advance related to straight and curved trajectories is reported for different τ and ψ . The values of d keep always lower than the length of the crack advance Δ (Eq.(1)), the condition $d/\Delta < 0.25$ being always satisfied except for high positive τ. Note also that when passing from $\tau = 0.3$ to $\tau = 0.4$ for mode I loading conditions ($\psi = 0°$), d diminishes due to the fact that for $\tau = 0.3$ the extension tends to curve (Fig. 4) but not to kink (according to both straight and curved extensions), whereas for $\tau = 0.4$ the straight extension assumption predicts $\theta_c \neq 0°$ (Fig.2).

3. Mode I loading conditions

Let us now focus our attention on pure mode I loading conditions ($K_{II} = 0$). For a kinked crack, if T is sufficiently large, $T \geq T_{th} > 0$, the crack ceases to propagate collinearly and the critical SIF deviates from the fracture toughness. Predictions according to the average stress criterion are depicted in Figs. 6 and 7. The threshold τ_{th} was estimated to be equal to 0.375, coherently with what found in Smith et al. (2001). The value differs from that obtained through FFM $\tau_{th} = 0.420$ (Cornetti et al., 2014) and that provided by Leguillon's approach $\tau_{th} = 0.704$ (Leguillon and Murer, 2008).

On the other hand, by assuming a curved crack, the critical SIF starts to deviate from the fracture toughness at a critical threshold $\tau_{th}^{a} = 0.229 < \tau_{th}$ (Fig.6). Thus, once again, the failure load related to a curved crack propagation reveals to be lower (or equal) than that corresponding to a straight trajectory. The maximum percent deviation can be quantified in nearly 6% over the whole range of analyzed τ. Furthermore, the trajectory starts to curve (with a null kinking angle, Fig. 7) for $\tau \geq \tau_{th}^{a}$ (Fig. 8). The curvature parameter can assume either positive or negative values, so that τ_{th}^{a} represents a bifurcation point. Note that a is a monotonic increasing function in τ. Finally, the angle γ_c deviates from 0° at $\tau_{th}^{\gamma} = 0.485$: this threshold influences also the behavior of a (Fig. 8). Due to symmetry, both positive or negative kinking angles are possible, corresponding to positive and negative curvatures, respectively.

4. Conclusions and discussion of results

The influence of T-stress on predictions by the average circumferential stress criterion was analyzed by considering a curved crack advance. It was shown that

for $T \neq 0$ a curved extension is always to be preferred than a straight one, since it corresponds to a lower failure load. Positive T-stresses originate a negative curvature parameter a, whereas negative T-stresses imply positive a. On the other hand, the variation of the kinking angle for curved cracks is less significant than for straight cracks: whereas (K_I, K_{II}) govern the singular stress field in front of the notch tip and thus the kinking angle as a local parameter, the contribution of T allows to describe the situation far from the notch root, outlining the effect on the curvature behavior. Besides τ, the curvature is also a function of the mode mixity and of the material. For mode I loading conditions and sufficiently high T ($\tau \geq \tau_{th}^{a} = 0.229$), the critical SIF deviates from the fracture toughness and the trajectory starts to curve, but not to kink yet. Only for higher τ ($\tau \geq \tau_{th}^{\gamma}$=0.485), the critical kinking angle assumes values different from $0°$. These results differ from those related to a straight extension, which provides a higher failure load (the mean percent deviation being around $4-5\%$) and a unique bifurcation point ($\tau_{th} = 0.375$).

In order to corroborate the present results, a comparison with experimental results would be suitable. Indeed, the task is not trivial due to many reasons. First of all, our analysis was limited to the propagation at the first step (the crack advance) and it did not cover a complete crack path. Secondly, most of the experimental works presented in the Literature considered the fracture load and the kinking angle, not measuring (although observed) the curvature. As a matter of fact, the distinction between the kinking angle and the curvature may be not a trivial task in the close vicinity of the crack tip. Eventually, the specific function chosen to model the present crack extension can be a limiting assumption.

Despite this, some general observations can be made. The function $y = ax^b$

represents the typical shape of mode II cracks under compression ($K_I = 0$), as described by Isaksson and Ståhle (2002). The investigation carried out in (Isaksson and Ståhle, 2002) on different tests on brittle rock-like materials (Shen et al., 1995; Bobet and Einstein, 1998) revealed an exponent b belonging to the range (1.43-1.58), and a curvature parameter comprised between 0.052 and 0.147. Since τ is negative, this is in fair agreement with what depicted in Fig. 4. Indeed, a complete analysis would require the inclusion of two components of T-stress (parallel and perpendicular to the crack plane, respectively), the interaction between the crack faces in contact and friction (see (Li et al., 2009; Tang, 2015)). In Smith et al. (2006) specific tests under mode II loading conditions were performed to investigate T-stress effects: PMMA specimens were broken under a positive T corresponding to $\tau_c \approx 0.26$ and negative T related to $\tau_c \approx -0.4$. The former specimens presented a slightly curved fracture, whereas in the second samples, the curvature was noteworthy. This is again described qualitatively by Fig. 4.

As concerns mode I loading conditions, Radon et al. (1977) preformed experiments on biaxially stressed PMMA sheets, observing that the curvature is an increasing function of τ, whereas the crack angle deviates from zero only above a threshold. Both positive or negative curvatures were measured, in correspondence to positive and negative kinking angles, respectively. These results agree with the present analysis (Section 3). Moreover, studies carried out in Selvarathinam and Goree (1998) and Chao et al. (2001) on PMMA specimens, showed very low thresholds for τ_{th} ($\tau_{th} \approx 0.07$ in Chao et al. (2001) assuming $\sigma_u = 70$Mpa, which differs significantly from that by the present criterion, and even more from those by the coupled criteria cited in Section 3). The curvature was not measured, but the observed initiation angles did not exceed the value of 30°. More recently, Ay-

atollahi et al. (2016) investigated the fracture trajectory of PMMA samples under pure mode I loading conditions. Five PMMA specimens of different shapes were tested, corresponding to τ=0.06, 0.1, 0.22, 0.24, and 0.25. The experimental critical kinking angle was zero for the former two geometries, and then it started to decrease. Note that τ=0.22 nearly coincides with the threshold τ_{th}^{a} computed in Section 3. Indeed, the curvature of the crack advance was not analyzed, but that related to the whole crack path was found to increase starting again from $\tau = 0.22$.

Finally, note that the present methodology can also be applied to predict onset of small curved cracks at singular points like single material and multi-material corners, an example being such cracks observed in experiments with bimaterial Brazilian disk specimens by Vicentini et al. (2012).

Acknowledgements

The financial support of V Plan Propio de Investigación de la Universidad de Sevilla (Modalidad I.6C), the Spanish Ministry of Economy and Competitiveness and European Regional Development Fund (Projects MAT2012-37387 and MAT2015-71036-P), the Junta de Andaluca and the European Social Fund (Project TEP-04051) are gratefully acknowledged. Eventually, Dr. Alberto Sapora acknowledges the hospitality of Universidad de Sevilla, where this work was mostly accomplished.

References

Amestoy, M., Leblond, J. B., 1992. Crack paths in plane situations -II. detailed form of the expansion of the stress intensity factors. International Journal of Solids and Structures 29, 465–501.

Ayatollahi, M. R., Rashidi-Moghaddam, M., Razavi, S. M. J., Berto, F., 2016. Geometry effects on fracture trajectory of pmma samples under pure mode-I loading. Engineering Fracture Mechanics, http://dx.doi.org/10.1016/j.engfracmech.2016.05.014, in press.

Ayatollahi, M. R., Torabi, A. R., 2010. Brittle fracture in rounded-tip V-shaped notches. Materials and Design 31, 60–67.

Ayatollahi, M. R., Torabi, A. R., Firoozabadi, M., 2015. Theoretical and experimental investigation of brittle fracture V-nocthed PMMA specimens under compressive loadings. Engineering Fracture Mechanics 135, 187–205.

Banichuk, N. V., 1970. Determination of the form of a curvilinear crack by small parameter technique. Izv. AN SSR, MTT (Mechanics of Solids) 7, 130–137 (in Russian).

Becker, T. L., Cannon, R. M., Ritchie, R. O., 2001. Finite crack kinking and T-stresses in functionally graded materials. International Journal of Solids and Structures 38, 5545–5563.

Bobet, A., Einstein, H. H., 1998. Fracture coalescence in rock-type materials under uniaxial and biaxial compression. International Journal of Rock Mechanics and Mining Sciences 35, 863–888.

Broberg, K. B., 1999. Cracks and Fracture. Academic Press, New York.

Carpinteri, A., Cornetti, P., Pugno, N., Sapora, A., 2011. The problem of the critical angle for edge and center V-notched structures. European Journal of Mechanics A/Solids 30, 281–285.

Carpinteri, A., Cornetti, P., Sapora, A., 2012. A finite fracture mechanics approach to the asymptotic behaviour of U-notched structures. Fatigue Fract Engng Mater Struct 35, 451–457.

Carpinteri, A., DiTommaso, A., Viola, E., 1979. Collinear stress effect on the crack branching phenomenon. Matériaux et Construction 12, 439–446.

Chao, Y. J., Liu, S., Broviak, B. J., 2001. Brittle fracture: Variation of fracture toughness with constraint and crack curving under mode I conditions. Experimental Mechanics 41, 232–241.

Cornetti, P., Sapora, A., Carpinteri, A., 2014. T-stress effects on crack kinking in finite fracture mechanics. Engineering Fracture Mechanics 132, 169–176.

Cotterell, B., 1972. Brittle fracture in compression. International Journal of Fracture Mechanics 8, 195–208.

Cotterell, B., Rice, J. R., 1980. Slightly curved or kinked cracks. International Journal of Fracture 16, 155–169.

Erdogan, F., Sih, G. C., 1963. On the crack extension in plates under plane loading and transverse shear. Journal of Basic Engineering 85, 519–525.

Finnie, I., Saith, A., 1973. A note on the angled crack problem and the directional stability of cracks. International Journal of Fracture 9, 484–486.

Goldstein, R. V., Salganik, R. L., 1970. Plane problem of curvilinear cracks in an elastic solid. Izv. AN SSR, MTT (Mechanics of Solids) 7, 69–82 (in Russian).

Gupta, M., Alderliesten, R. C., Benedictus, R., 2015. A review of T-stress and its effects in fracture mechanics. Engineering Fracture Mechanics 134, 218–241.

He, M. Y., Bartlett, A., Evans, A. G., Hutchinson, J. W., 1991. Kinking of a crack out of an interface: Role of in-plane stress. Journal of the American Ceramic Society 74, 767–771.

Isaksson, P., Ståhle, P., 2002. Mode II crack paths under compression in brittle solids a theory and experimental comparison. International Journal of Solids and Structures 39, 2281–2297.

Jayadevan, K. R., Narasimhan, R., Ramamurthy, T. S., Dattaguru, B., 2001. A numerical study of T-stress in dynamically loaded fracture specimens. International Journal of Solids and Structures 38, 4987–5005.

Kariahaloo, B. L., 1982. On crack kinking and curving. Mechanics of Materials 1, 189–201.

Karihaloo, B. L., Keer, L. M., Nemat-Nasser, S., Oranratnachai, A., 1981. Approximate description of crack kinking and curving. ASME J. Appl. Mech. 48, 515–519.

Leevers, P. S., Radon, J. C., 1982. Inherent stress biaxiality in various fracture specimen geometries. International Journal of Fracture 19, 311–315.

Leguillon, D., 2002. Strength or toughness? A criterion for crack onset at a notch. European Journal of Mechanics A/Solids 21, 61–72.

Leguillon, D., Murer, S., 2008. Crack deflection in a biaxial stress state. International Journal of Fracture 150, 75–90.

Li, D. F., Li, C. F., Qing, H., Lu, J., 2010. The elastic T-stress for slightly curved or kinked cracks. International Journal of Solids and Structures 47, 1753–1763.

Li, X. F., Liu, G. L., Lee, K. Y., 2009. Effects of T-stresses on fracture initiation for a closed crack in compression with frictional crack faces. International Journal of Fracture 160, 19–30.

Li, X. F., Xu, L. R., 2007. T-stress across static crack kinking. Journal of Applied Mechanics 74, 181–190.

Melin, S., 2002. The influence of the T-stress on the directional stability of cracks. International Journal of Fracture 114, 259–265.

Neuber, H., 1958. Theory of Notch Stresses. Springer, Berlin.

Novozhilov, V., 1969. On a necessary and sufficient condition for brittle strength. Prik Mat Mek 33, 212–222.

Priel, E., Bussiba, A., Gilad, I., Yosibash, Z., 2007. Mixed mode failure criteria for brittle elastic V-notched structures. Int J Fract 144, 247–265.

Radon, J. C., Lever, P. S., Culver, L. E., 1977. Fracture Toughness of PMMA Under Biaxial Stress, in Fracture 1977, Vol. 3. University of Waterloo Press, Waterloo, Canada.

Salvadori, A., 2008. A plasticity framework for (linear elastic) fracture mechanics. Journal of the Mechanics and Physics of Solids 56, 2092–2116.

Sapora, A., Cornetti, P., Carpinteri, A., 2013. A finite fracture mechanics approach to V-notched elements subjected to mixed-mode loading. Engineering Fracture Mechanics 97, 216–226.

Sapora, A., Cornetti, P., Carpinteri, A., 2014. V-notched elements under mode II loading conditions. Structural Engineering and Mechanics 49, 499–508.

Sapora, A., Mantič, V., 2016. Finite fracture mechanics: a deeper investigation on negative T-stress effects. International Journal of Fracture 197, 111–118.

Selvarathinam, A. S., Goree, J. G., 1998. T-stress based fracture model for crack in isotropic materials. Engineering Fracture Mechanics 60, 543–561.

Seweryn, A., 1994. Brittle fracture criterion for structures with sharp notches. Engineering Fracture Mechanics 47, 673–681.

Seweryn, A., 1998. A non-local stress and strain energy release rate mixed mode fracture initiation and propagation criteria. Engineering Fracture Mechanics 59, 737–760.

Seweryn, A., Lukaszewicz, A., 2002. Verification of brittle fracture criteria for elements with V-shaped notches. Engineering Fracture Mechanics 69, 14877–1510.

Shen, B., Stephansson, O., Einstein, H. H., Ghahreman, B., 1995. Coalescence of fractures under shear stresses in experiments. Journal of Geophysical Research 100, 5795–5990.

Smith, D. J., Ayatollahi, M. R., Pavier, M. J., 2001. The role of T-stress in brittle fracture for linear elastic materials under mixed-mode loading. Fatigue Fract Engng Mater Struct 24, 137–150.

Smith, D. J., Ayatollahi, M. R., Pavier, M. J., 2006. On the consequences of T-stress in elastic brittle fracture. Proceedings of the Royal Society A 462, 2415–2437.

Sumi, Y., Nemat-Nasser, S., Keer, L. M., 1985. On crack path stability in a finite body. Engineering Fracture Mechanics 22, 759–771.

Tang, S. B., 2015. The effect of T-stress on the fracture of brittle rock under compression. International Journal of Rock Mechanics and Mining Sciences 79, 286–98.

Taylor, D., 2007. The Theory of Critical Distances: A New Perspective in Fracture Mechanics. Elsevier, Oxford, UK.

Taylor, D., Merlo, M., Pegley, R., Cavatorta, M., 2004. The effect of stress concentrations on the fracture strength of polymethylmethacrylate. Mater Sci Engng A 382, 288–294.

Vicentini, D., Barroso, A., Justo, J., Mantič, V., París, F., 2012. Determination of generalized fracture toughness in composite multimaterial closed corners with two singular terms part II: Experimental results. Engineering Fracture Mechanics 89, 15–23.

Williams, J. G., Ewing, P. D., 1972. Fracture under complex stress - the angled crack problem. International Journal of Fracture Mechanics 8, 441–446.

Yang, B., Ravi-Chandar, K., 2001. Crack path instabilities in a quenched glass plate. J Mech Phys Solids 49, 91–130.

List of Figures

1 Cracked element with a kinked curvilinear crack of length Δ. . . . 21

2 Straight crack propagation: effects of the dimensionless T-stress, ranging from -0.4 to 0.4 with a step equal to 0.1, on the critical kinking angle θ_c (deg). The dashed line refers to the case $\tau = 0$. . 22

3 Effects of the dimensionless T-stress, ranging from -0.4 to 0.4 with a step equal to 0.1, on the fracture loci: straight crack propagation (continuous lines) and curved crack propagation (dashed lines). The thick dashed line refers to the case $\tau = 0$. 23

4 Effects of the dimensionless T-stress, ranging from -0.4 to 0.4 with a step equal to 0.1, on the dimensionless critical curvature parameter. The dashed line refers to the case $\tau = 0$, whereas the circles represent the stationary points. 24

5 Effects of the dimensionless T-stress on the critical kinking angle γ_c (deg). The dashed line refers to the case $\tau = 0$. 25

6 Average stress predictions for mode I loading conditions : T-stress effects on the critical the failure load according to a straight crack advance (continuous line) and a curved crack advance (thick continuous line). 26

7 Average stress predictions for mode I loading conditions : T-stress effects on the critical kinking angle (deg) according to a straight crack advance (continuous line) and a curved crack advance (thick continuous line). 27

8 Average stress predictions for mode I loading conditions : T-stress effects on the dimensionless critical curvature parameter. . . 28

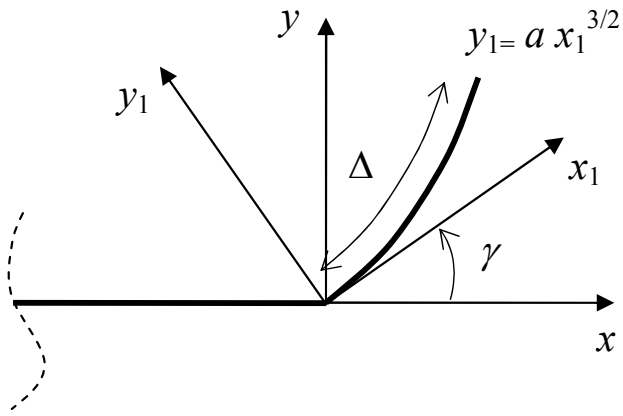

Figure 1: Cracked element with a kinked curvilinear crack of length Δ.

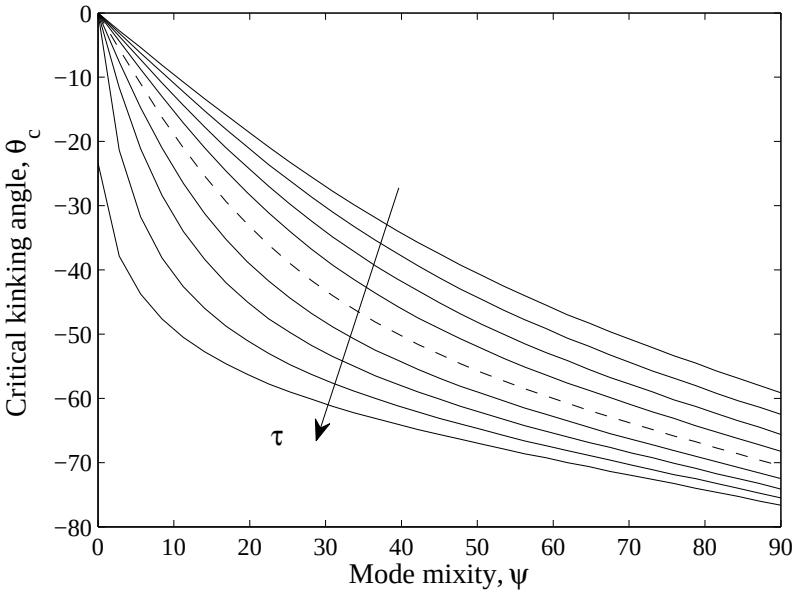

Figure 2: Straight crack propagation: effects of the dimensionless T-stress, ranging from -0.4 to 0.4 with a step equal to 0.1, on the critical kinking angle θ_c (deg). The dashed line refers to the case $\tau = 0$.

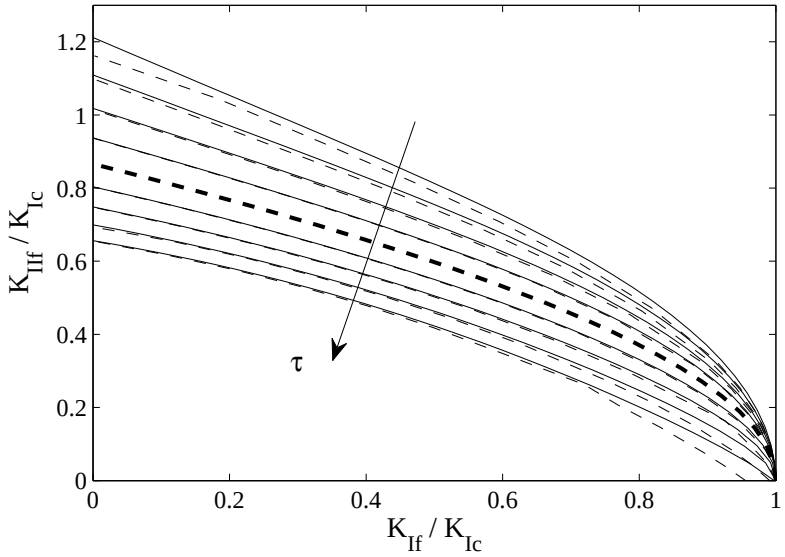

Figure 3: Effects of the dimensionless T-stress, ranging from -0.4 to 0.4 with a step equal to 0.1, on the fracture loci: straight crack propagation (continuous lines) and curved crack propagation (dashed lines). The thick dashed line refers to the case $\tau = 0$.

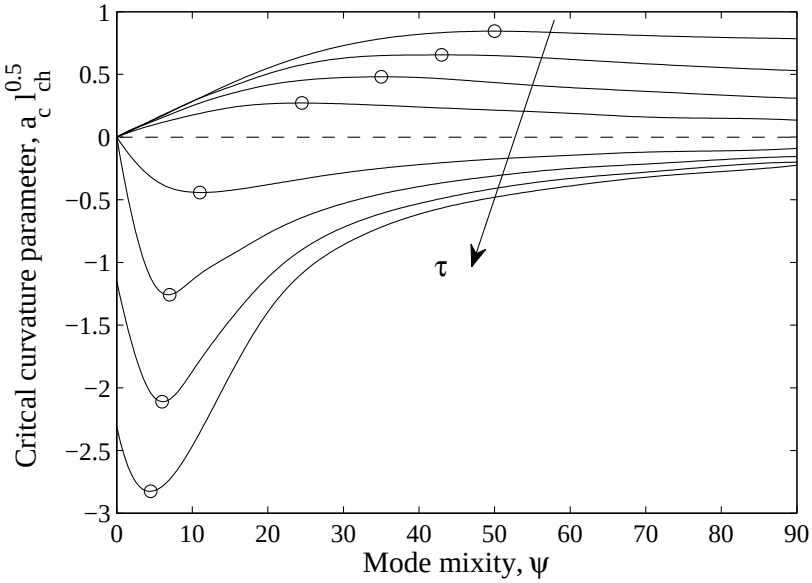

Figure 4: Effects of the dimensionless T-stress, ranging from -0.4 to 0.4 with a step equal to 0.1, on the dimensionless critical curvature parameter. The dashed line refers to the case $\tau = 0$, whereas the circles represent the stationary points.

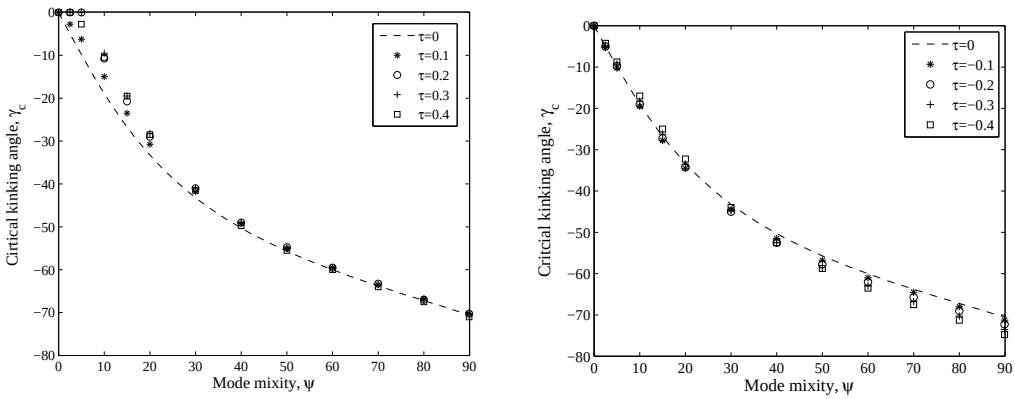

Figure 5: Effects of the dimensionless T-stress on the critical kinking angle γ_c (deg). The dashed line refers to the case $\tau = 0$.

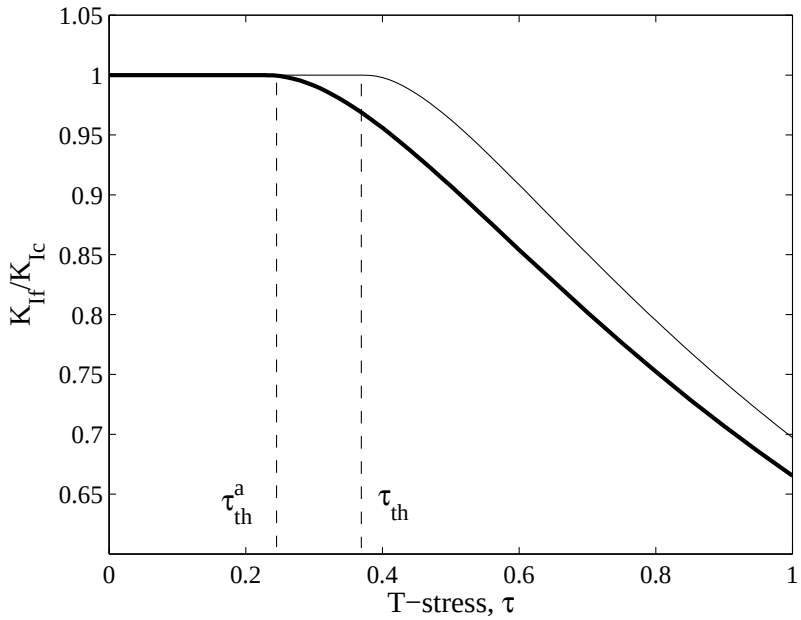

Figure 6: Average stress predictions for mode *I* loading conditions : *T*-stress effects on the critical the failure load according to a straight crack advance (continuous line) and a curved crack advance (thick continuous line).

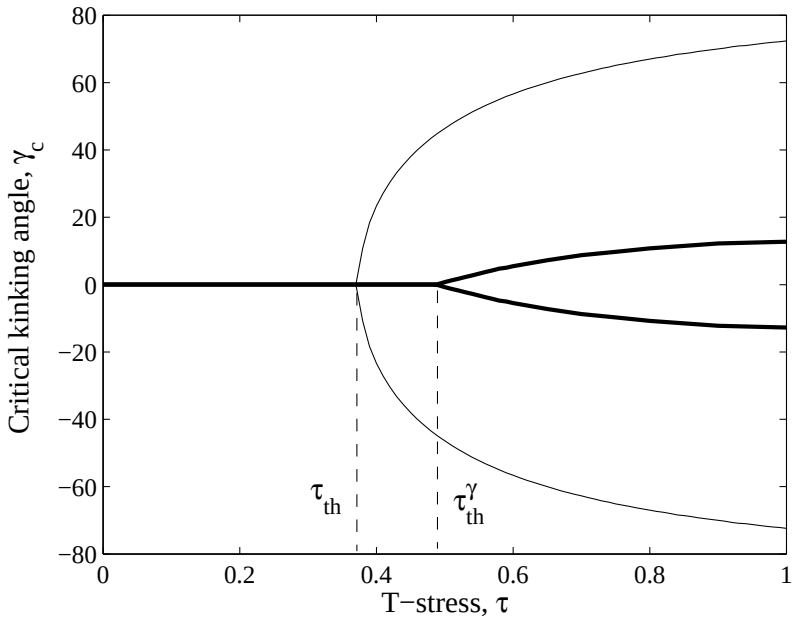

Figure 7: Average stress predictions for mode *I* loading conditions : *T*-stress effects on the critical kinking angle (deg) according to a straight crack advance (continuous line) and a curved crack advance (thick continuous line).

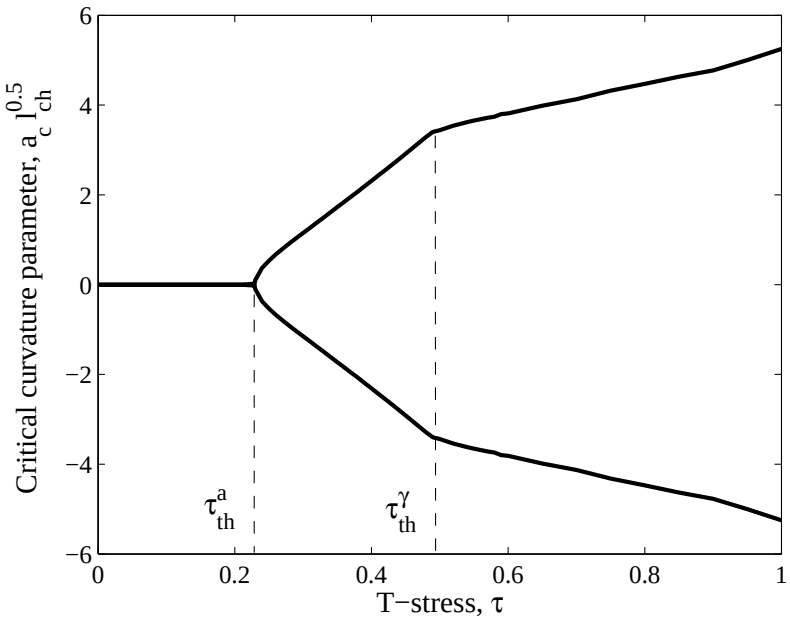

Figure 8: Average stress predictions for mode *I* loading conditions : *T*-stress effects on the dimensionless critical curvature parameter.

List of Tables

1 Dimensionless distance d/l_{ch} between the end points of curved and straight crack advances. 30

$\psi \setminus \tau$	-0.4	-0.3	-0.2	-0.1	0.1	0.2	0.3	0.4
0°	0.000	0.000	0.000	0.000	0.000	0.000	0.419	0.337
30°	0.128	0.121	0.101	0.063	0.069	0.112	0.133	0.140
60°	0.152	0.129	0.092	0.048	0.035	0.059	0.075	0.081
90°	0.159	0.122	0.078	0.035	0.021	0.035	0.044	0.049

Table 1: Dimensionless distance d/l_{ch} between the end points of curved and straight crack advances.